Available online at www.sciencedirect.com
SCIENCE DIRECT®
Journal of Sound and Vibration 267 (2003) 621–635
JOURNAL OF SOUND AND VIBRATION
www.elsevier.com/locate/jsvi

A comparison of a theoretical model for quasi-statically and dynamically induced environmental vibration from trains with measurements

X. Sheng*, C.J.C. Jones, D.J. Thompson

Institute of Sound and Vibration Research, University Southampton, Highfield, Southampton SO17 1BJ, UK

Accepted 9 May 2003

Abstract

This paper presents comparisons between a theoretical ground vibration model and measured data at three sites. The model, which is briefly outlined here, encompasses both the quasi-static and dynamic mechanisms of excitation. The vertical dynamics of a number of vehicles travelling at a constant speed on an infinite track are coupled to a semi-analytical model for a three-dimensional layered ground. This model is also used to demonstrate the roles of the two components of vibration at different frequencies and for train speeds below and above the lowest ground wave speed. It is found that, in most practical cases, the dynamic component gives rise to the higher level of vibration.

1. Introduction

The problem of ground vibrations generated by surface trains has received great attention in the past few years. A seminar focussing on this problem was held in March 2000 at Gothenburg, Sweden [1]. At this seminar, about 50 researchers from different countries exchanged their experiences on the topic. At the WAVE 2000 Workshop [2] in Bochum, Germany, a large proportion of the papers were devoted to ground vibration from railway trains. A number of models have therefore been reported for predicting ground vibrations from trains (e.g., [3–6]). The new interest lies particularly in high-speed lines where train speeds may exceed the propagation velocities of waves in soft soils. Thus, amongst the three sources of excitation [6], which are moving axle (quasi-static) loads, stationary dynamic forces and moving dynamic forces, most of

*Corresponding author. Tel.: +44-23-8059-2311; fax: +44-23-8059-3190.
E-mail address: xzs@isvr.soton.ac.uk (X. Sheng).

0022-460X/$ - see front matter
doi:10.1016/S0022-460X(03)00728-4

the models only take into account the first, i.e., the moving axle loads. For environmental vibration, however, it is still the case that slow heavy-axle load traffic on conventional lines gives rise to the majority of complaints about vibration in line-side buildings. Ground vibration induced by moving axle loads is independent of the dynamics of vehicles and of track quality. It is known that, at least in some circumstances, these do have an effect on the level of vibration. In fact, Lai et al. [7] show that consideration of only quasi-static loads underestimates the actual response level, especially for higher excitation frequencies.

The dynamic excitations at wheel–rail contact points come from the irregular vertical profiles of the wheel and the rail running surfaces. The variations in the vertical profiles of either surface introduce a relative displacement input to the vehicle and track systems. A wavelength λ generates a frequency of excitation $f = c/\lambda$, where c denotes the train speed. For the frequency range of 5–80 Hz of interest for ground vibration and a train speed range of 36–250 km/h (10–70 m/s), the important wavelengths lie within the range of 0.125–14 m (or wave number from 0.07 to 8 cycle/m).

Comprehensive analysis requires realistic models of ground vibration generation and propagation. These models should be able to account for the interactions between vehicles, track and ground, and for the effect of train speeds. Such a model has been developed by the present authors. This paper, having briefly outlined the model (Section 2), compares vibration predictions from this model with measured data at three sites (Sections 3–5). A more detailed description for the predictions and comparisons can be found in Ref. [8]. The comparisons show a reasonable correspondence. The model is also used to demonstrate the roles of the two components of vibration at different frequencies and for train speeds below, and above, the lowest ground wave speed.

2. Outline of the model

The model consists of three subsystems: vehicles, a track and a ground. Each vehicle is modelled as a multi-body system (Fig. 1) but only vertical dynamics are considered. As shown in Fig. 1, M_C and J_C denote the mass and the pitch inertia of the car body, and M_B and J_B denote those of each bogie. Boxes containing a cross represent the suspensions. The frequency-dependent dynamic

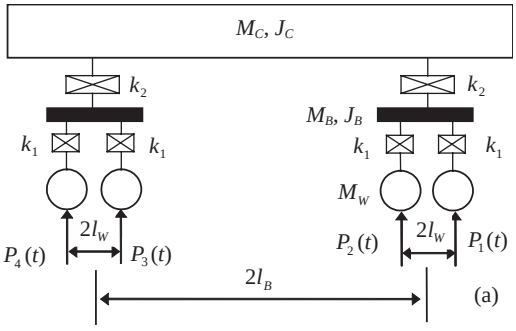

Fig. 1. The model for a bogied vehicle.

stiffness of the secondary suspension per bogie is denoted by k_2, while that of the primary suspension per axle is denoted by k_1. For each wheelset, M_W denotes its mass.

The model for the railway track, presented in Fig. 2, is the same as that used in Ref. [6]. From the first wheelset of the first vehicle to the last wheelset of the last vehicle, the vertical wheel–rail forces are denoted by $P_1(t), P_2(t), \ldots, P_M(t)$, where M is the number of these forces. At time $t = 0$, the longitudinal co-ordinates of these forces are denoted by $a_1, a_2, \ldots, a_M$. Each wheel–rail force consists of two components, the moving axle load and the moving dynamic load excited by the combined wheel–rail irregularities. The vertical displacement of the rail is denoted by $w_R(x, t)$.

As in Ref. [6], the ground may consist of a number, n, of layers. Underneath the nth layer a homogeneous half-space or a rigid foundation may be present. For particles on the ground surface, the vertical (z-direction) displacement is denoted by $w_{10}(x, y, t)$. When a unit vertical harmonic load of angular frequency Ω is applied at the rails and moves at speed c (when $t = 0$, the x-coordinate of the load position is zero), the steady-state displacements of the rails and the ground surface may be expressed as

$$\begin{aligned} w_R(x, t) &= w_R^{\Omega}(x - ct)\mathrm{e}^{\mathrm{i}\Omega t}, \\ w_{10}(x, y, t) &= w_{10}^{\Omega}(x - ct, y)\mathrm{e}^{\mathrm{i}\Omega t}. \end{aligned} \tag{1}$$

For a single wavelength of rail irregularity, λ, the vehicles vibrate at frequency $\Omega = 2\pi c/\lambda$, and the wheel–rail forces can be expressed as $P_l(t) = \tilde{P}_l(\Omega)\mathrm{e}^{\mathrm{i}\Omega t}$, where $l = 1, 2, \ldots, M$. The responses of the rails and the ground surface due to this rail irregularity are given by summing those induced by each wheel–rail force, i.e.,

$$\begin{aligned} w_R(x, t) &= \textstyle\sum_{k=1}^{M} w_R^{\Omega}(x - a_k - ct)\tilde{P}_k(\Omega)\mathrm{e}^{\mathrm{i}\Omega t}, \\ w_{10}(x, y, t) &= \textstyle\sum_{k=1}^{M} w_{10}^{\Omega}(x - a_k - ct, y)\tilde{P}_k(\Omega)\mathrm{e}^{\mathrm{i}\Omega t}. \end{aligned} \tag{2}$$

From Eq. (2), the amplitude of the displacement of the lth wheel/rail contact point on the rails, denoted by $\tilde{z}_{Rl}(\Omega)$, is given by letting $x = a_l + ct$ in Eq. (2):

$$\tilde{z}_{Rl}(\Omega) = \sum_{k=1}^{M} \sigma_{lk}^{R}\tilde{P}_k(\Omega), \tag{3}$$

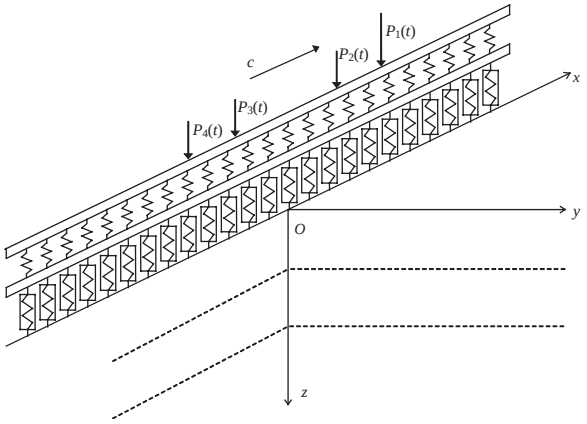

Fig. 2. The track-ground system model.

where

$$\sigma_{lk}^{R} = w_{R}^{\Omega}(a_l - a_k) \tag{4}$$

which is the transfer receptance between the lth and the kth wheel/rail contact point on the rails and due to the motion of the loads, $\sigma_{lk}^{R} \neq \sigma_{kl}^{R}$.

Similarly, the displacement amplitude of the lth wheelset, denoted by $\tilde{z}_{Wl}(\Omega)$, can be expressed as

$$\tilde{z}_{Wl}(\Omega) = \sum_{k=1}^{M} \sigma_{lk}^{T} \tilde{P}_k(\Omega), \tag{5}$$

where σ_{lk}^{T} is determined by the parameters of the vehicles and is the transfer receptance between the lth wheelset and the kth wheelset, and $\sigma_{lk}^{T} = \sigma_{kl}^{T}$.

It is assumed that each wheelset is always in contact with the rails. This requires that

$$\sum_{k=1}^{M} (\sigma_{lk}^{T} + \sigma_{lk}^{R})\tilde{P}_k(\Omega) + \tfrac{1}{k_{Hl}} \tilde{P}_l(\Omega) = -\tilde{z}_l(\Omega) \quad (l = 1, 2, \ldots, M), \tag{6}$$

where k_{Hl} denotes the stiffness of the Hertz contact spring between the lth wheelset and the rails, and $\tilde{z}_l(\Omega)$ denotes the amplitude of the rail irregularity of the wavelength considered. From Eq. (6) the wheel/rail forces can be calculated. Thus the displacements of the track and the ground surface are completely determined by Eq. (2).

The displacement spectra of the rails and the ground surface are obtained by performing Fourier transformation on Eq. (2) with respect to time t. In Eq. (6), let $\tilde{z}_l(\Omega) = 1$. Then the vertical displacement spectrum of point (x, y) on the ground surface is denoted by $S_w(x, y, f; \Omega)$, where f is the frequency at which the spectrum is evaluated. The vertical irregular profile of the rails is normally described by its power spectral density (PSD) $P_z(\beta)$, where β denotes the wave number in radians. For each wave number of a discrete spectrum of the rail irregularity, the displacement spectrum of the ground can be evaluated as described above. The total displacement spectrum of the ground is equal to the sum of those for each wave number of the rail irregularity. It can be shown that the total vertical displacement power spectrum on the ground surface, denoted by $P_w(x, y, f)$, is given by

$$P_w(x, y, f) = |S_w(x, y, f; 0)|^2 + \frac{1}{2\pi} \sum_{k=1}^{\infty} \{|S_w(x, y, f; \Omega_k)|^2 + |S_w(x, y, f; -\Omega_k)|^2\} P_z(\beta_k) \Delta\beta, \tag{7}$$

where, $\beta_k = k\Delta\beta$, $\Omega_k = \beta_k c$. In Eq. (7), the first part corresponds to the power spectrum generated by the quasi-static loads while the second part is due to the track irregularity. When divided by a chosen period of time, which normally is the time needed for the whole train to pass a fixed point, Eq. (7) gives an estimation of the vertical displacement PSD of the ground surface.

3. Simulations and comparison for site I: Ledsgård

In this section, the model is applied to the vibrations from the X2000 high-speed train at a site called Ledsgård [1] where the Swedish National Rail Administration (Banverket) encountered very large vibrations when the trains operated at 200 km/h. Banverket carried out an extensive

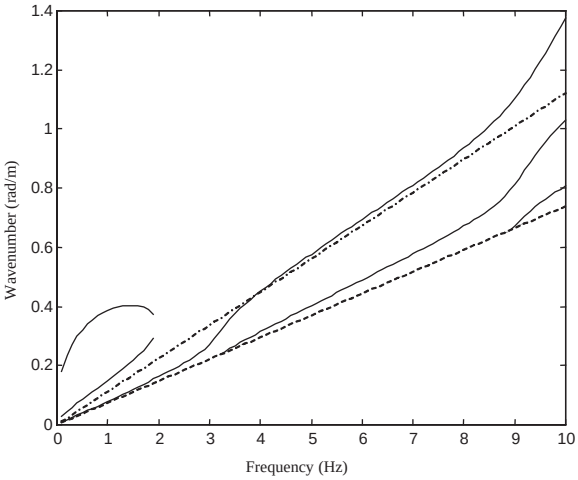

Fig. 3. Dispersion curves of the ground at Ledsgård. ——, P-SV modes; – – –, shear wave of the half-space; – · – · –, the load speed line for a speed of 55.6 m/s.

programme of measurements using a test train to investigate the causes [9]. The ground at this site is modelled here as two layers on a homogeneous half-space using properties identified in Ref. [9]. The first layer is 1.1 m deep with P- and S-wave speeds of 500 and 65 m/s. The second layer, 3 m deep, is very soft 'organic clay' with P- and S-wave speeds of 500 and 32 m/s. The underlying half-space has wave speeds of 1500 and 85 m/s. The track is on an embankment about 1 m high and has monobloc concrete sleepers in ballast.

Fig. 3 shows the dispersion curves of propagating P-SV modes of vibration predicted for the ground at Ledsgård. The dispersion curves describe the free vibration of the ground, giving the dependence of propagating wave number on frequency. A complex characteristic of the ground is revealed by this figure. Below 2 Hz, three wave types exist, while between 2 and 3.3 Hz only one exists. To show which waves are excited by a surface load, the Fourier transformed displacement on the ground surface due to a vertical unit point load of discrete frequencies between 0 and 50 Hz is presented in Fig. 4. This figure indicates that only modes with wave speeds higher than the Rayleigh wave speed in the first layer (62 m/s) but lower than the shear wave speed in the underlying half-space, are excited on the surface. Other waves propagate along the interface of the second layer and the half-space but decay rapidly with vertical distance away from the interface so that they do not contribute significantly to the surface response. Therefore only when a load moves at a speed close to the Rayleigh wave speed of the surface layer, is the ground surface expected to have a strong response.

3.1. Displacements of the track generated by the quasi-static loads

Calculations have been carried out for the vibration displacements generated by the axles of the whole X2000 test train at 70 km/h (19.4 m/s) and 200 km/h (55.6 m/s). Figs. 5 and 6 show the instantaneous displacements of the embankment for the two train speeds. At the track, the response to the dynamic wheel–rail forces is small compared to that due to the quasi-static loads.

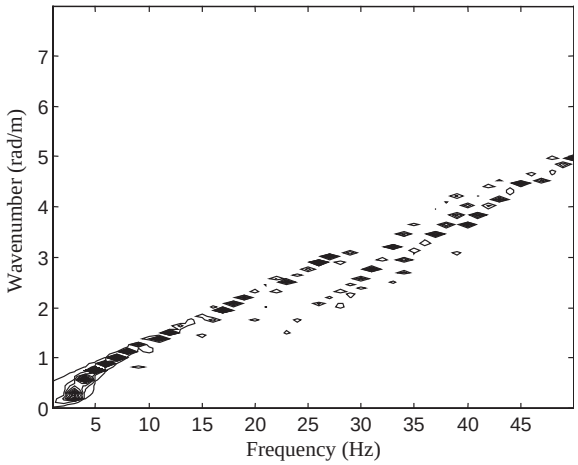

Fig. 4. Contour plot of the Fourier transformed vertical displacement on the ground surface at Ledsgård.

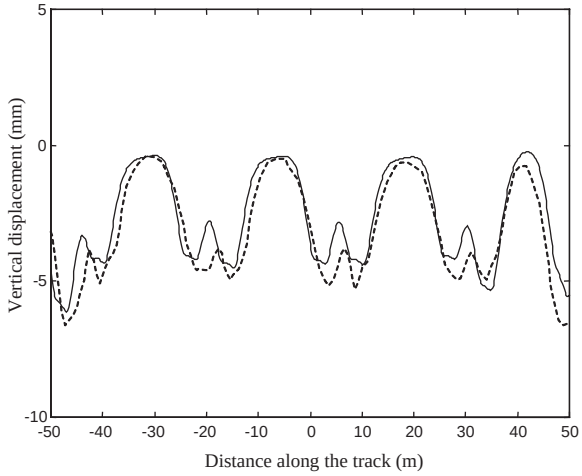

Fig. 5. Predicted (——) and measured (– – –) vertical displacement of the embankment under the X2000 train running at 70 km/h (19.4 m/s).

The success of the prediction indicates the accuracy of the ground and track parameters derived by Banverket. For the low-speed case shown in Fig. 5, a quasi-static loading state is indicated. However, in the high-speed case, since a propagating wave mode is excited, an oscillating response appears with a much higher amplitude. The excitation due to load moving at 200 km/h (55.6 m/s) is indicated in Fig. 3 by a straight line. It has an intersection with the dispersion curve of the first mode at wave number 0.4 rad/m (4 Hz). The presence of the mass of the track and embankment (not included in the calculation of the dispersion curves) decreases the wave number of this intersection slightly. As a result, a propagating wave of about 16 m wavelength is excited. This propagates along the track from each load and can be seen in Fig. 6 as an oscillation continuing after the last axle load has passed.

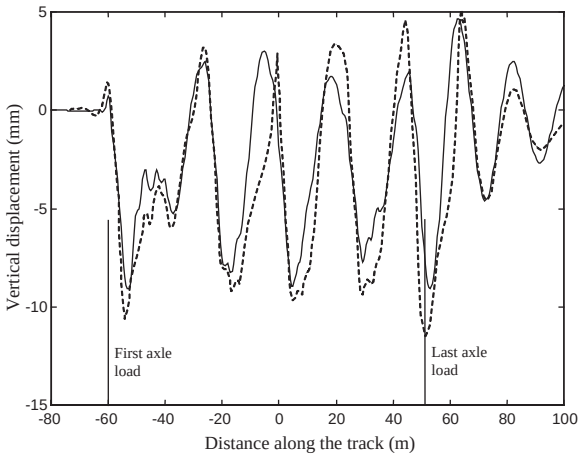

Fig. 6. Predicted (——) and measured (– – –) vertical displacement of the embankment under the X2000 train running at 200 km/h (55.6 m/s).

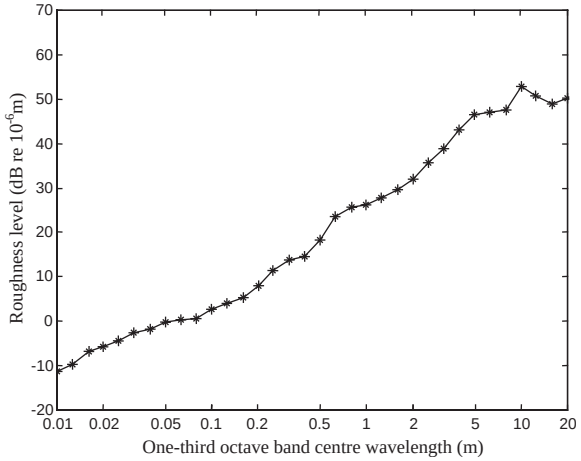

Fig. 7. Rail roughness/vertical profile from measurements on mixed traffic 200 km/h line in the UK, used in the predictions for sites I and II.

3.2. *Vibration velocity spectra due to both quasi-static and dynamic loads*

The total response generated by the test train has been predicted on the basis of vehicle suspension parameters provided by Banverket and, in the absence of site-specific data, a typical rail profile spectrum measured on 200 km/h, mixed-traffic main line in England (Fig. 7) has been used. The vertical velocity levels of two points (7.5 and 15 m from the track) on the ground surface for the two train speeds are shown in Figs. 8–11. Figs. 8 and 9, for the case in which the train speed is lower than the wave speeds in the ground, show that the dynamic components of the wheel–rail forces are dominant over the quasi-static loads even for very low frequencies. However, in Figs. 10 and 11, for the train at 200 km/h, exceeding the wave speeds in the ground, the

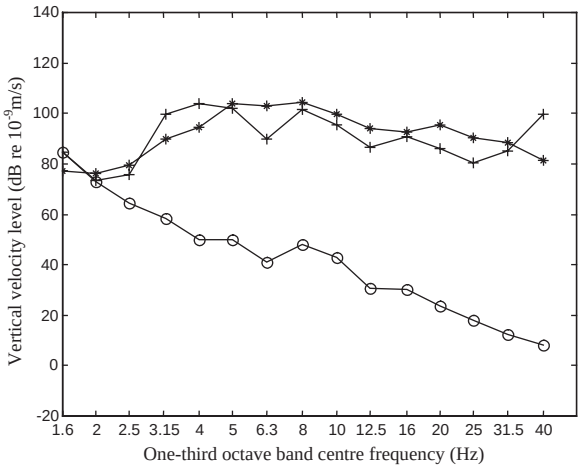

Fig. 8. Vertical velocity level for train speed of 70 km/h (19.4 m/s) at 7.5 m (○, predicted level due to quasi-static loads; +, predicted total level; *, measured level).

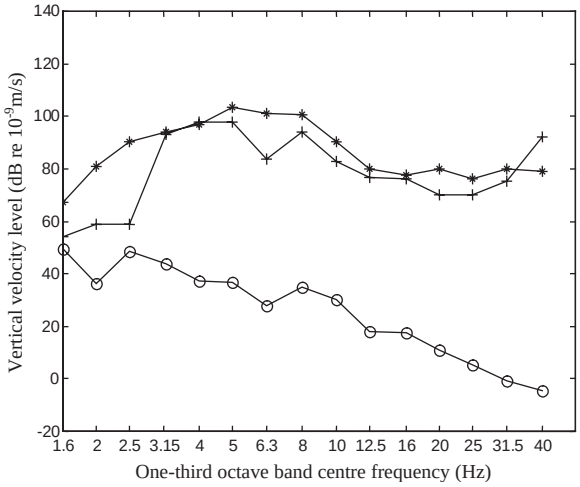

Fig. 9. Vertical velocity level for train speed of 70 km/h (19.4 m/s) at 15 m from the track on the ground surface (○, predicted level due to quasi-static loads; +, predicted total level; *, measured level).

response from the quasi-static loads dominates particularly for the frequency range where the load speed excites the first mode (about 3–9 Hz, Fig. 3).

4. Simulations and comparison for site II: Via Tedalda

In this section, measured and predicted vibrations are compared for the ETR500 high-speed train at Via Tedalda in Italy [7]. The average speed of the train passages during the measurement was about 70–80 km/h. The vibration has been measured at two points, 13 and 26 m from the

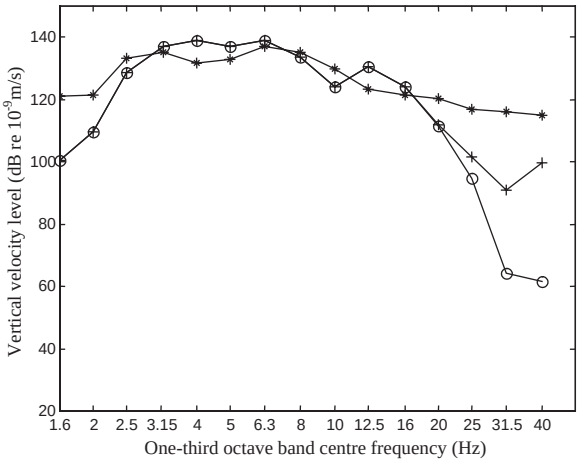

Fig. 10. Vertical velocity level for train speed of 200 km/h (55.6 m/s) at 7.5 m from the track on the ground surface (○, predicted level due to quasi-static loads; +, predicted total level; *, measured level).

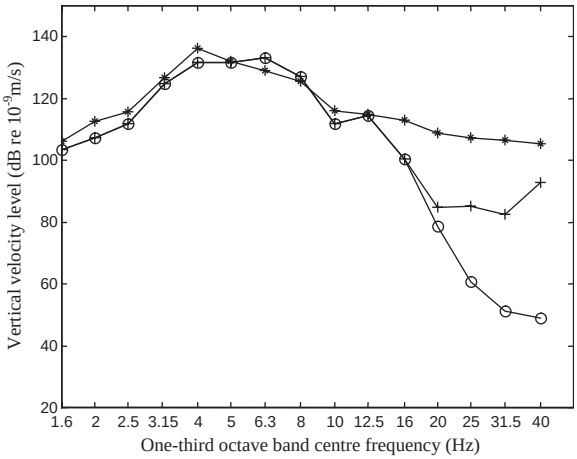

Fig. 11. Vertical velocity level for train speed of 200 km/h (55.6 m/s) at 15 m from the track on the ground surface (○, predicted level due to quasi-static loads; +, predicted total level; *, measured level).

track. Using Fig. 5 in Ref. [7], a model of the ground as one layer of 10 m depth overlying a homogenous half-space has been produced. The P- and S-wave speeds in the layer are identified as 995 and 300, and 1990 and 600 m/s in the half-space. The dispersion curves of the ground are shown in Fig. 12. The first cut-on frequency in the layer is 11.2 Hz, at which a second propagating mode occurs.

In the absence of specific parameters, the track structure, other than the embankment, has been assigned parameters typical of a ballasted track with monobloc sleepers. The embankment is 1.5 m high, and its density has been estimated as 1800 kg/m^3. Since Young's modulus of the embankment is uncertain, several values have been tested. Fig. 13 compares predicted and measured vibration (acceleration) spectra at a point 13 m from the track and Fig. 14, at a point

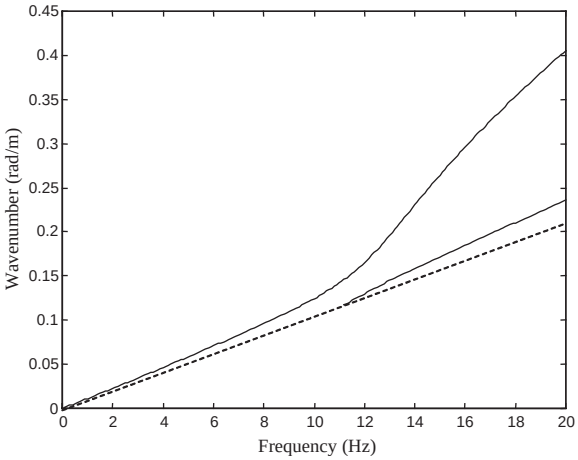

Fig. 12. Dispersion curves of P-SV (——) waves in the ground and the shear wave of the underlying half-space (– – –) for site II.

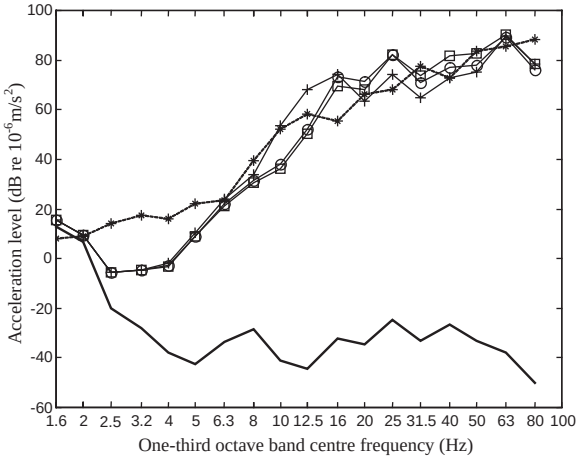

Fig. 13. Effect of embankment Young's modulus on vertical acceleration levels 13 m from the track at Via Tedalda when five ETR 500 cars run at 25 m/s (+, 2×10^7 N/m^2; ○, 5×10^7 N/m^2; □, 10×10^7 N/m^2; *, measured [7]; ▬, predicted level due to quasi-static loads).

26.2 m from the track. The effects of the variation in Young's modulus of the embankment are shown in these two figures. The results show that the value of embankment Young's modulus (20 MN/m^2) giving the closest correspondence with measurement is that derived from the total vertical stiffness of the track, 50.5 MN/m^2, suggested in Ref. [7]. In the calculations, five ETR500 passenger cars running at 25 m/s are coupled with the track-ground system and, again in the absence of specific data, the rail profile spectrum shown in Fig. 7 has been used.

Figs. 13 and 14 show a rise in vibration level corresponding to the cut-on at about 11 Hz. A close agreement is achieved for frequencies higher than 5 Hz. However for frequencies of 2–5 Hz, the predicted levels are much lower than the measured ones. It is possible that this is due, in part, to a building near the track (Fig. 4 in Ref. [7]). Three frequency ranges are identified in Figs. 13

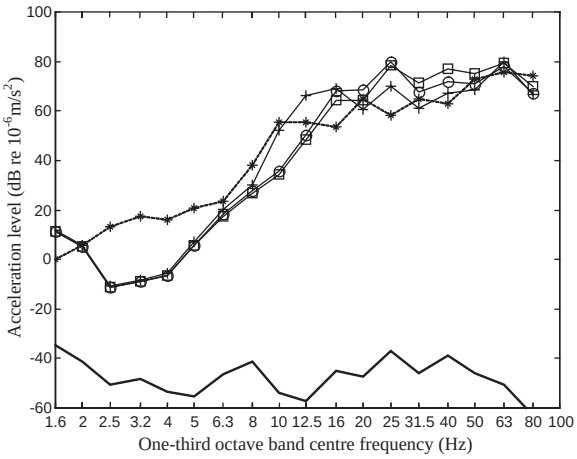

Fig. 14. Effect of embankment Young's modulus on vertical acceleration levels 26.2 m from the track at Via Tedalda when five ETR 500 cars run at 25 m/s (+, 2×10^7 N/m^2; ○, 5×10^7 N/m^2; □, 10×10^7 N/m^2; *, measured [7]; ▬, predicted level due to quasi-static loads).

and 14: 1.6–5, 5–16 and 16–80 Hz. The response level does not depend on the embankment stiffness in the first frequency range but decreases with increasing embankment stiffness in the second frequency range and increases in the third. The figures also show the response due to the quasi-static loads without the dynamic mechanism. Clearly, in this case, the dynamic components of the wheel–rail forces dominate the response.

5. Simulations and comparison for site III: Burton Joyce

Vibration spectra induced by a train of two-axle freight wagons (type HAA) forms the third comparison. Information on the measurement at Burton Joyce in Nottinghamshire, England is reported in Ref. [10]. The average speed of trains during the measurement was about 14 m/s. The ground is modelled as a single layer of 1.8 m depth, overlying a homogenous half-space using the parameters suggested in Ref. [10]. The P- and S-wave speeds in the layer are 341, 81, 1700 and 216 m/s in the half-space. Fig. 15 presents the dispersion curves for the propagating waves for this soil.

The track is ballasted with an embankment of 1.3 m height. In this case, site specific rail profile measurements from the time of the vibration measurements are available. This is presented in Fig. 16. The transfer mobility (vertical response due to vertical load) from the track to the ground surface was measured by British Rail Research. Fig. 17 shows this and the mobility calculated using the present model. The calculation and measurements are similar in character as well as level and both show a strong rise at a frequency of about 10 Hz. This is a lower frequency than the cut-on of the first propagating mode at about 15 Hz (Fig. 15) because of the influence of the track/embankment structure.

Fig. 18 shows the predicted vertical velocity levels on the ground 10 m from the track for different embankment Young's moduli and different track/ground contact widths. Also shown in bold lines are the maximum and minimum measured levels from several trains. Since the ground is

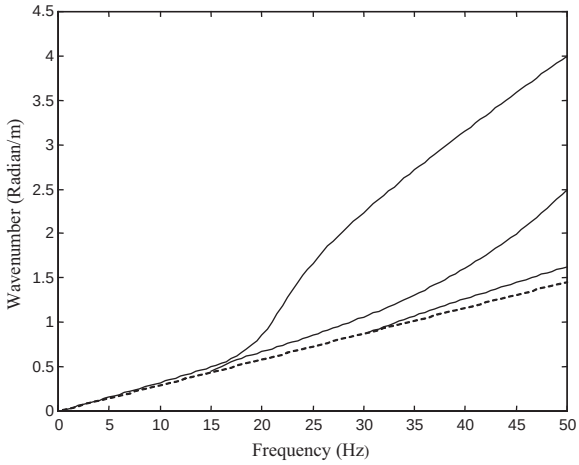

Fig. 15. Dispersion curves of P-SV (——) waves in the ground and the shear wave of the underlying half-space (– – –) for site III.

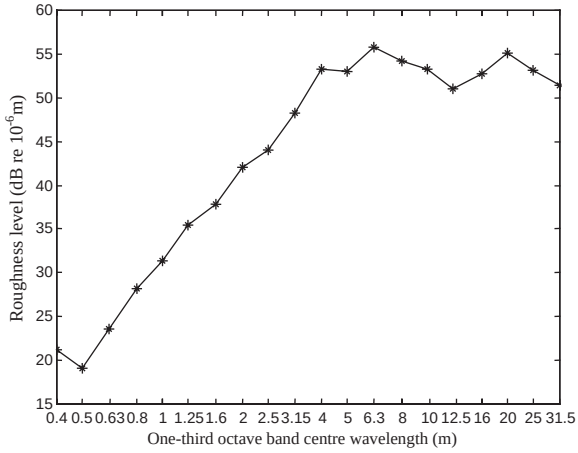

Fig. 16. Rail vertical profile measurements made specifically for site III.

relatively soft, modification of the track parameters has a great effect on the response levels for frequencies higher than 10 Hz. The level of response due to the quasi-static loads is less than 40 dB and therefore not shown in the figure.

6. Discussion

The prediction of train-induced ground vibration has been carried out for three sites. The dynamically induced vibration prediction requires the knowledge of the vehicle dynamics and measurements of the vertical profile of the track. Site-specific data for the latter was only available to the authors for the third site. For the first two sites typical data have been used.

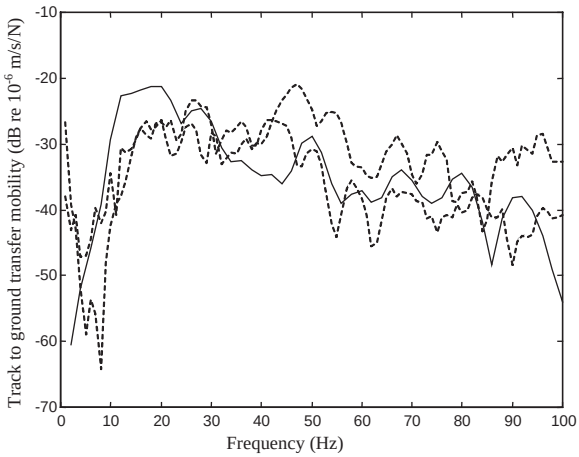

Fig. 17. Transfer mobility from track to ground surface (vertical component) at a distance of 10 m from the near rail at site III (——, predicted; – – –, measured, two results measured at sites about 20 m apart along track).

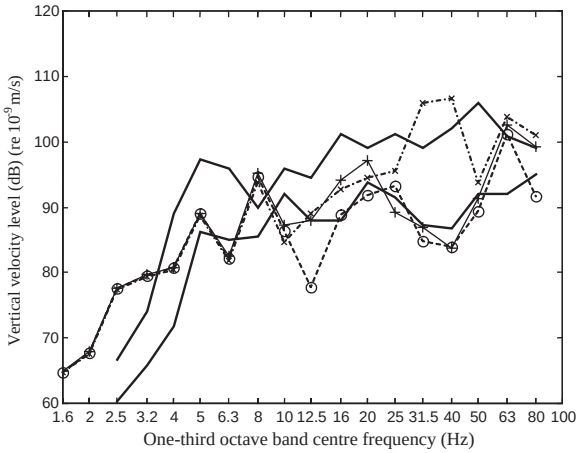

Fig. 18. Vertical velocity levels at 10 m from the track at site III when five wagons run at 14 m/s (+, embankment Young's modulus = 1.5×10^7 N/m^2, track/ground contact width = 4 m; ○, embankment Young's modulus = 1.5×10^7 N/m^2, track/ground contact width = 5 m; ×, embankment Young's modulus = 3×10^7 N/m^2, track/ground contact width = 4 m; *, maximum and minimum measured levels).

At the first site, Ledsgård, the ground is not only unusually soft, but also unusual in that the second layer is softer than the surface layer. The measured displacement at the track has been shown to be close to that predicted for the quasi-static loads of the train both in the case of the train speed below, and above, the speed of the wave in the ground/embankment (Figs. 5 and 6). For the lower train speed (70 km/h), the dynamically induced vibration dominates the spectrum of vibration on the ground surface away from the track (Figs. 8 and 9). However, when the train speed exceeds the wave speed in the ground, a much higher level of vibration is observed and the quasi-statically induced vibration dominates. The highest levels of transmitted vibration are from

3 to 8 Hz corresponding to the excitation of the first propagating mode of the soil (Fig. 3). The predicted level of the dynamically induced vibration appears to be too low at high frequency in Figs. 10 and 11. This may in part be due to the fact that the prediction is based on typical vertical profile data and may not be appropriate for a track that has been subjected to high dynamic displacements.

The second site, Via Tedalda, is very different from Ledsgård being a relatively stiff soil. The model predicts the rise in the measured vibration level that occurs in the frequency range from about 8 to 16 Hz (Figs. 13 and 14) due to the cut-on of the propagating wave at 11 Hz (Fig. 12). The measurements at this site are for a train speed that is lower than the first mode of propagation in the ground. For the measurement distances at 13 and 26 m from the track, the observed vibration is demonstrated to be due to the dynamic generation mechanism. The stiffness of the embankment is not known and results show that the predicted levels are sensitive to this parameter for the frequency range in which propagation takes place in the upper layer (and the track). Notwithstanding the uncertainty in the embankment stiffness and the vertical track profile data, the model predicts the vibration level well for most of the frequency range except for 2.5–5 Hz. No satisfactory explanation for the under-prediction in this range has been found.

At the first two sites, measurements were made for modern passenger rolling stock. Measurements for two-axle freight wagons were made at the third site, Burton Joyce. Here, there are fairly soft soil conditions with the speed of the first propagating wave in the ground tending towards 77 m/s at high frequency (i.e. the 'Rayleigh' wave speed). As well as the specifically measured vertical profile of the track, measurements of transfer mobility for the ground [10] and from the track to the ground (Fig. 17) are available. These confirm that the ground model and track/ground model show good agreement with the measurement data at intermediate stages before the comparison of measurements of train-induced vibration. With some uncertainty in the parameters for the embankment and the effective width that should be used for the contact of the track structure with the ground, the levels predicted are close to, or within, the band of measured levels (Fig. 18). This suggests that a much closer correspondence with predictions than those obtained from the model would not be significant. The predicted level due to the quasi-static loads is much lower than the measured levels. Thus in the vibration observed at this site, the dynamically induced component of vibration is, once more, the dominant one.

7. Conclusions

The comparisons of measured and predicted vibration at three sites show the model to be valid for a wide range of ground conditions and vehicle types and the role of uncertainties in the parameters is confirmed. Where the train travels below the speed of wave propagation in the ground, the results presented here show that the dynamic mechanism of vibration generation is considerably more important than the quasi-static axle loads for environmental vibration. For the X2000 train at 200 km/h at Ledsgård, the excitation of a propagating wave by the quasi-static axle loads is confirmed.

Acknowledgements

The authors are grateful to A. Smekal and Dr. M. Li of the Swedish National Rail Administration (Banverket), Dr. C. G. Lai (Studio Geotecnico Italiano S.r.l., Milano, Italy) and J. Block (AEA Technology, UK) and their organizations for the provision of parameters and measured data.

References

[1] Banverket, *Seminar on High Speed Lines on Soft Ground, Dynamic Soil-Track Interaction and Groundborne Vibration*, The Swedish National Railway Authority, Banverket, Gothenburg, Sweden, 2000.
[2] N. Chouw, G. Schmid, *Proceedings of Wave* 2000, Balkema, Rotterdam, 2000.
[3] V.V. Krylov, Calculation of low frequency vibrations from railway trains, *Applied Acoustics* 42 (1994) 199–213.
[4] M. Petyt, C.J.C. Jones, Modelling of ground-borne vibration from railways, *Structural Dynamics-EURODYN'99*, 1999, pp. 79–87.
[5] H. Grundmann, M. Lieb, E. Trommer, The response of a layered half-space to traffic loads moving along its surface, *Archive of Applied Mechanics* 69 (1) (1999) 55–67.
[6] X. Sheng, C.J.C. Jones, M. Petyt, Ground vibration generated by a load moving along a railway track, *Journal of Sound and Vibration* 228 (1) (1999) 129–156.
[7] C.G. Lai, A. Callerio, E. Faccioli, A. Martino, Mathematical modelling of railway-induced ground vibrations, *Proceedings of the International Workshop Wave* 2000, 2000, pp. 99–110.
[8] X. Sheng, C.J.C. Jones, D.J. Thompson, A comparison of a theoretical model for quasi-statically and dynamically induced environmental vibration from trains with measurements, ISVR Technical Memorandum No. 865, 2001.
[9] Banverket, High-speed line on soft ground, Report, 1998 (in Swedish).
[10] C.J.C. Jones, J.R. Block, Prediction of ground vibration from freight trains, *Journal of Sound and Vibration* 193 (1) (1996) 205–213.